



OPEN ACCESS

EDITED BY
Da Xie,
Shanghai Jiao Tong University, China

REVIEWED BY
Srete Nikolovski,
Josip Juraj Strossmayer University of
Osijek, Croatia
Amit Kumar,
Thapar Institute of Engineering &
Technology, India

*CORRESPONDENCE
Chen Jie,
xj_cj@163.com

SPECIALTY SECTION
This article was submitted to Smart
Grids,
a section of the journal
Frontiers in Energy Research

RECEIVED 08 August 2022
ACCEPTED 30 August 2022
PUBLISHED 05 January 2023

CITATION
Yujing H, Jie C, Xueqin T and Yafei W
(2023), Integrated photovoltaic storage
joint smoothing strategy based on
simultaneous perturbation stochastic
approximation algorithm.
Front. Energy Res. 10:1014027.
doi: 10.3389/fenrg.2022.1014027

COPYRIGHT
© 2023 Yujing, Jie, Xueqin and Yafei.
This is an open-access article
distributed under the terms of the
[Creative Commons Attribution License
\(CC BY\)](https://creativecommons.org/licenses/by/4.0/). The use, distribution or
reproduction in other forums is
permitted, provided the original
author(s) and the copyright owner(s) are
credited and that the original
publication in this journal is cited, in
accordance with accepted academic
practice. No use, distribution or
reproduction is permitted which does
not comply with these terms.

Integrated photovoltaic storage joint smoothing strategy based on simultaneous perturbation stochastic approximation algorithm

He Yujing¹, Chen Jie^{1,2*}, Tian Xueqin³ and Wang Yafei¹

¹School of Electrical Engineering, Xinjiang University, Urumqi, China, ²School of Electrical Engineering, Shanghai Dian Ji University, Shanghai, China, ³State Grid Economic and Technological Research Institute Co., Ltd, Beijing, China

In order to realize the real-time control of photovoltaic power generation smoothly connected to the grid under the condition that the energy storage equipment can operate safely, a control strategy combining the simultaneous perturbation stochastic approximation (SPSA) algorithm with rule control is designed. Firstly, the photovoltaic data are processed to extract the data characteristics of the power ramp, and then the grid-connected reference power is obtained through SPSA algorithm. Secondly, considering the state of charge (SOC) of energy storage equipment and the safe operating power range of hydrogen storage equipment, 24 hybrid energy storage power allocation rules are formulated by using the rule control method. Finally, according to the sampling data of every 10 s interval in typical day, the simulation is carried out on MATLAB/simulink platform. The results show that, compared with the first-order low-pass filtering algorithm and recursive fuzzy neural network (RFNN) algorithm, the SPSA algorithm has stronger smoothing ability, and the rule control can also complete the allocation according to the characteristics of the hybrid storage device while ensuring its normal operation.

KEYWORDS

photovoltaic power generation, hybrid energy storage, simultaneous perturbation stochastic approximation, rule control, energy management strategy

1 Introduction

China's government has clearly put forward the target of carbon peak in 2030 and carbon neutrality by 2060, and the proportion of non-fossil energy in primary energy consumption has increased significantly. Solar energy is a kind of renewable energy with abundant resources, wide distribution and no pollution (Nigam and Sharma, 2021). In 2020, the cumulative installed photovoltaic capacity in the world was 767.2 GW, which was significantly higher than that of 39.2 GW in 2010. Therefore, it is imperative to continue to develop ultra-large scale and ultra-high proportion of photovoltaic renewable clean energy.

However, photovoltaic power generation depends on weather parameters, such as solar irradiance, so it has strong intermittence and randomness in nature (Shaner et al., 2018). The conflict between the controllability of the non-sourced side and the high dynamics load is more prominent (Bharti et al., 2022). In order to solve this problem, experts and scholars have proposed a more flexible solution, which combines photovoltaic power generation with energy storage systems to eliminate the fluctuations of active power (Akbari et al., 2019). Energy storage systems is a widely accepted solution because most of them are geographically independent and controllable in different time frames (Castillo and Dennice 2014). The power conditioning system composed of hydrogen storage and super-capacitor is one of the ways (Bharti et al., 2022). This energy storage system belongs to the category of hybrid energy storage, which can reduce environmental costs, improve response time, energy conversion efficiency and durability. Combining a large-scale photovoltaic power generation systems with hybrid energy storage systems can significantly alleviate the uncertain random power generation challenges in power grid operation and planning (Puranen et al., 2021).

The rapid growth of photovoltaic power generation in the past few years has promoted the demand for robust energy management strategies, which take into account the specific technical features and limitations of different storage devices (Wang et al., 2021). Most of the previous off-line power management strategies assumed perfect forecast of renewable energy, demand and markets, which is difficult to achieve in practice (Li 2021). Appropriate on-line energy management strategy can balance the power of a hybrid energy system, improving system reliability and system efficiency, reducing production costs, prolonging the life of system components (Y. Wu et al., 2018). As far as technical, economic and social standards are concerned, the stochastic strategy surpasses the deterministic method, and it has high potential for real-time power management strategies (S. Yin et al., 2021). In (P. Li et al., 2020), the Lyapunov drift-plus-penalty function is applied to formulate a relaxed form of the energy management problem, more effectively taking into account the uncertainty of energy storage and power load. Tabar et al. (2019) presents the application of stochastic linear programming method in the energy management of hybrid micro-gridncertain systems considering multiple markets and rereal-timeemand response. Using this method can effectively reduce the cost, pollution and demand payment of micro-grid.

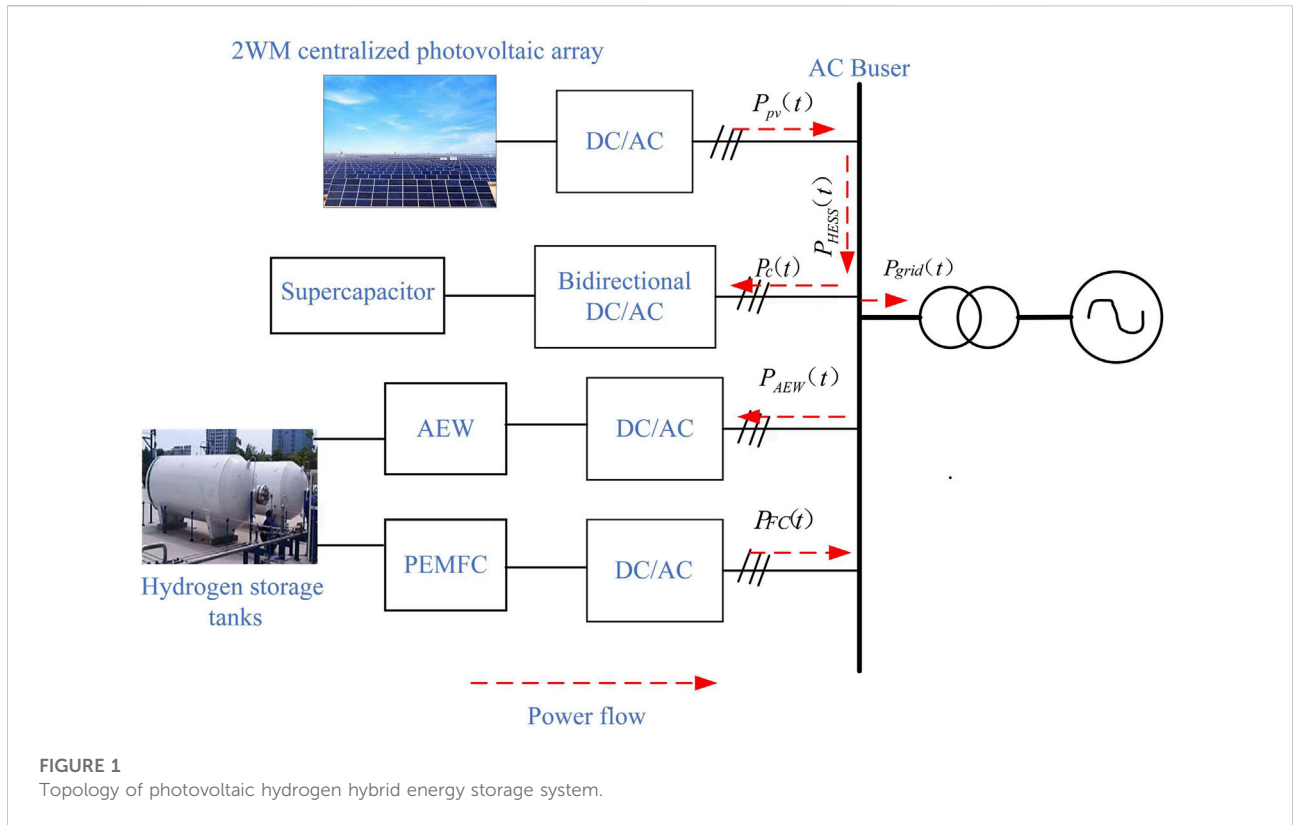
Common stochastic methods include stochastic game theory algorithm, stochastic linear programming algorithm, Lyapunov optimization algorithm, and SPSA algorithm (Ciupageanu, Barelli et al., 2020). Among them, Liapunov optimization algorithm and SPSA algorithm are gradient-based stochastic algorithm, can adapt to the time-varying environment without mandatory uncertainty modeling in the process of real-time energy management (Neely 2010). In the past, most of the

articles used real-time energy management methods based on Liapunov optimization algorithm, while the smoothing strategy of photovoltaic power generation based on SPSA algorithm is not common. What's more, most of the previous articles are aimed at the single-objective or multi-objective optimization of a single online control algorithm. few articles combine the online control based on optimization algorithm with the control strategy based on rules, and apply them to the energy distribution process of hybrid energy storage, which can smooth the fluctuations and considering the characteristics of the equipment. These articles can not consider the operation characteristics of the energy storage equipment more flexibly. For example (Barelli et al., 2020), smoothes the fluctuation of wind power generation based on the stochastic approximation of simultaneous disturbance combined with a flywheel-battery storage system, but its constraint target is not suitable for the safe operation conditions of hydrogen storage. Hydrogen storage devices can realize medium and long-term storage, and the hybrid storage system composed of this devices and super-capacitors has more unique requirements on operational safety than the previous hybrid storage system composed of batteries and super-capacitors.

Therefore, a strategy of photovoltaic output fluctuation smoothing and power distribution based on SPSA algorithm and rule control is proposed. Firstly, the SPSA algorithm is applied to smooth the photovoltaic output at the system level, the result is compared with the smoothing results of the first-order low-pass filtering algorithm and the RFNN algorithm during the result verification, the smoothness drop to 0.3418 in the verification, which effectively suppresses the fluctuations. Secondly, in the energy allocation of the hybrid energy storage system, considering the SOC of the energy storage system and the power constraint of the hydrogen storage equipment, 24 rules are established for the energy allocation of the hybrid energy storage system, so that the hydrogen storage equipment can operate within the safe power constraint on the basis of giving full play to the respective advantages of energy-based and power-based equipment, so as to avoid the explosion accident caused by the excess hydrogen in oxygen.

2 Grid-connected photovoltaic hydrogen hybrid storage coupling system topology diagram

The combination of integrated photovoltaic systems and hybrid energy storage devices can reduce the active power imbalance of power grid regulation, improve the stability of power grid and increase the penetration rate of new energy. In this paper, the photovoltaic power station adopts a common AC bus topology, and the energy storage system consists of alkaline electrolyzed water (AEW), hydrogen storage tank, proton exchange membrane fuel cell (PEMFC), and super capacitor, as shown in Figure 1.



The energy balance equation is shown below.

$$P_{pv}(t) = P_{grid}(t) + P_{HESS} \tag{1}$$

$$P_{HESS}(t) = P_c(t) + P_H(t) \tag{2}$$

Where: $P_{pv}(t)$ is the active power emitted by the photovoltaic array at the moment t , $P_{grid}(t)$ is the power received by the grid at the moment t , $P_{HESS}(t)$ is the power allocated to the energy storage system at the moment t . $P_c(t)$ and $P_H(t)$ is the power allocated by the energy storage system to the super-capacitor and hydrogen storage system respectively, and the units of the above power are kW.

2.1 Modeling of hybrid energy storage equipment

This paper only considers the charging and discharging behavior and capacity limitation of energy storage devices, so it only discuss the relationship between charging and discharging power and SOC.

2.1.1 Operating characteristics and constraints of super-capacitor

In order to make the capacitor work in a normal state, the output power of the supercapacitor needs to be corrected with the SOC (Zhang et al., 2018). The expression is shown as follows:

$$SOC_c(i + 1) = SOC_c(i) + \frac{P_c(i) * \Delta t}{E_{c\max} * \eta_D} \tag{3}$$

$$SOC_c(i + 1) = SOC_c(i) + \frac{P_c(i) \eta_{ch} * \Delta t}{E_{c\max}} \tag{4}$$

$SOC(i + 1)$ and $SOC(i)$ denotes the SOC at moment t and moment $t+1$ respectively; $E_{c\max}$ denotes the maximum capacity of super-capacitor; η_C is the charging efficiency, which is taken as 0.95, and η_D is the discharging efficiency, which is taken as 0.95. $P_c(t)$ is the power allocated to super-capacitor at moment t , which is taken as positive when charging and negative when discharging. Δt is the sampling time.

2.1.2 Operational characteristics and constraints of hydrogen storage system

In this paper, the pressure of the high-pressure hydrogen storage tank is used to describe the SOC of the hydrogen storage system (Wang and Lin, 2019), The expressions of hydrogen flow rate in electrolyzer and fuel cell are as follows.

$$N_C = \eta_{AEW} \frac{P_{AEW}(t)}{2FU_{AEW}(t)} \tag{5}$$

$$N_D = \frac{1}{\eta_{FC}} \frac{P_{FC}(t)}{2FU_{FC}(t)} \tag{6}$$

N_C is the hydrogen flow rate during charging, and N_D is the hydrogen flow rate during discharging. η_{AEW} is the charging

efficiency and η_{FC} is the discharging efficiency. $P_{AEW}(t)$ is the charging power of electrolytic tank and $P_{FC}(t)$ is the discharging power of fuel cell. F is the Faraday constant. $U_{AEW}(t)$ is the voltage of the electrolyzer and $U_{FC}(t)$ is the voltage of the fuel cell.

The equation for the SOC is shown as follows.

$$\Delta P_C(t) = \frac{N_C(t) \cdot \Delta t \cdot RT}{V} \quad (7)$$

$$\Delta P_D(t) = \frac{N_D(t) \cdot \Delta t \cdot RT}{V} \quad (8)$$

$$\Delta P_G(t) = P_G(t-1) + \Delta P_C(t) - \Delta P_D(t) \quad (9)$$

$$SOC_H(t) = \frac{P_G(t)}{P_{Hmax}} \times 100\% \quad (10)$$

$\Delta P_C(t)$ is the increase in the pressure of the hydrogen storage tank and $\Delta P_D(t)$ is the decrease in the pressure of the hydrogen storage tank. R is the universal time constant, T is the gas temperature, and V is the volume of the hydrogen storage tank. $\Delta P_G(t)$ is the change in the total pressure of the hydrogen storage tank and $P_G(t-1)$ is the total pressure of the tank at the previous moment. $SOC_H(t)$ is the SOC of the hydrogen storage tank. P_{Hmax} is the maximum pressure that the hydrogen storage tank can withstand.

3 Photovoltaic power fluctuation smoothing strategy

3.1 Photovoltaic power data processing

In this paper, we take the of historical photovoltaic data of a certain place in China for example to analyze. This data includes two datasets: the first dataset is the sampling data of a centralized 2 MW photovoltaic power generation from January to July 4th at 5 min intervals. The second set of data is the sampling data every 10 s from 4:00 to 19:00 on a certain day in June.

The power slope ΔP is a measure of the photovoltaic power fluctuation, which can be expressed as the difference between the current power and the previous power. In order to use the algorithm for online control, it is necessary to use mathematical statistics and reasoning methods to find the data characteristics of the power ramp, so as to predict the value of the next second during real-time control. We averaged the daily power ramps for in the sample, and obtained the confidence intervals for the average and standard deviation for all sample points by fitting a normal distribution curve, as shown in Figure 2.

According to the fitted results, the average value of power ramp is 29.7353 kW (26.6837,32.787) at 95% confidence interval, and the standard deviation is 20.6894 kW (18.7452,23.087) at 95% confidence interval. This data feature will be described in the following SPSA algorithm by the cost function.

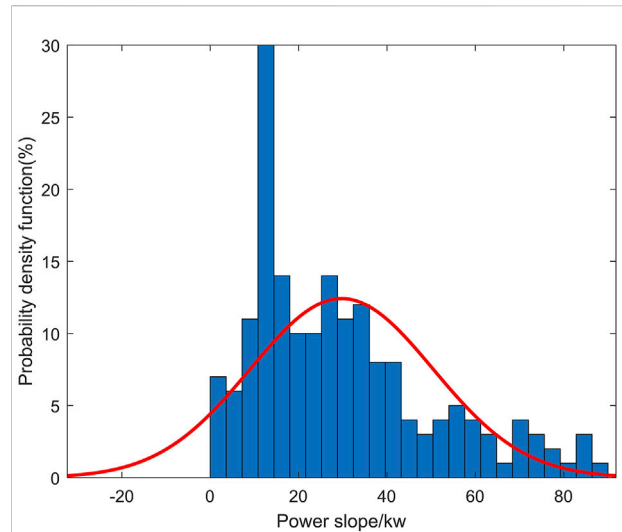


FIGURE 2
Probability density function of the power ramp.

3.2 Fluctuation smoothing strategy

In the process of smoothing the fluctuation of photovoltaic processing, this paper divides the control system into two parts: system level and equipment level, and the upper level is the lower level to output reference signals, as shown in Figure 3.

In this paper, we use the SPSA algorithm at the system level to calculate the power $P_{grid}(t)$ that satisfies the grid connection criteria after smoothing and the power $P_{HESS}(t)$ of the hybrid energy storage. The power of the hybrid energy storage device is allocated at the device level using the rule control algorithm.

3.2.1 Description of the simultaneous perturbation stochastic approximation algorithm

The input and output of the stochastic system are random signals. The stochastic approximation algorithm constructs stochastic recursive formulas based on the input and output data and uses the observed values to estimate the extreme values of the unknown function; this algorithm does not require *a priori* knowledge of the system model, i.e., it does not need to know the specific form of the cost function (Mokkadem and Pelletier, 2007).

The SPSA algorithm was put forward by Spall in 1992. In each gradient approximation, the SPSA algorithm only needs two measurements of the objective function, which is easy to implement and effective compared to other stochastic approximation algorithms (Spall, 1997). Compared with intelligent optimization-seeking algorithms such as finite difference, simulated annealing, and genetic algorithms, the SPSA algorithm is more robust to stochastic signals in the

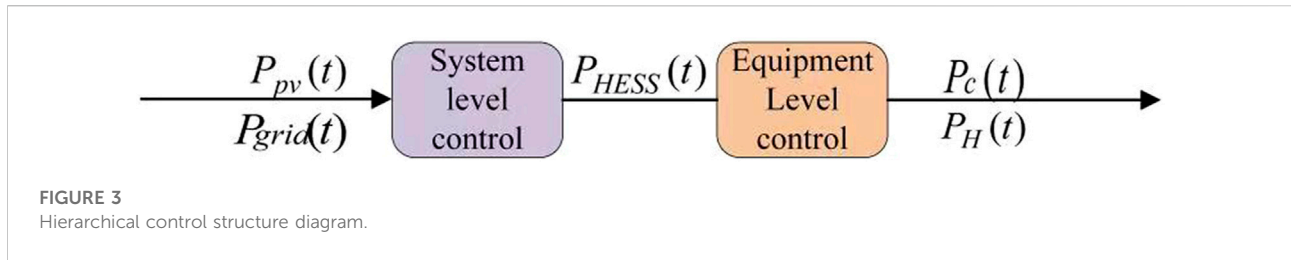


FIGURE 3 Hierarchical control structure diagram.

measurement of the cost function and has a stronger ability to find the global optimal solution.

Introduce a sequence of independent identical distributions with zero mean

$$\Delta_k = [\Delta_{k1}, \dots, \Delta_{kp}]^T \tag{11}$$

Calculate the value of the cost function g (10) at $\theta_k \pm c_k \Delta_k$, as shown in the following equation.

$$y_k^{(+)} = L(\theta_k + c_k \Delta_k) + \xi_k^{(+)} \tag{12}$$

$$y_k^{(-)} = L(\theta_k - c_k \Delta_k) + \xi_k^{(-)} \tag{13}$$

$\xi_k^{(+)}, \xi_k^{(-)}$ is the measurement noise term.

The gradient is estimated as

$$\hat{g}_k(\hat{\theta}_k) = \begin{bmatrix} \frac{y_k^{(+)} - y_k^{(-)}}{2c_k \Delta_{k1}} \\ \frac{y_k^{(+)} - y_k^{(-)}}{2c_k \Delta_{k2}} \\ \dots \\ \frac{y_k^{(+)} - y_k^{(-)}}{2c_k \Delta_{kp}} \end{bmatrix} = \frac{y_k^{(+)} - y_k^{(-)}}{2c_k} \begin{bmatrix} \frac{1}{\Delta_{k1}} \\ \frac{1}{\Delta_{k2}} \\ \dots \\ \frac{1}{\Delta_{kp}} \end{bmatrix} \tag{14}$$

The form of the SPSA algorithm is as follows.

$$\theta_{k+1} = \theta_k - a_k \hat{g}_k(\hat{\theta}_k) \tag{15}$$

The gain coefficient a_k, c_k , which can be obtained from the following equation.

$$a_k = \frac{a}{(k + A)^\alpha} \tag{16}$$

$$c_k = \frac{c}{k^\gamma} \tag{17}$$

3.2.2 Application of simultaneous perturbation stochastic approximation algorithm at system level

In order to smooth the fluctuation of photovoltaic power, this paper adopts the method of minimizing the power ramp of the next second grid-connected power relative to the photovoltaic power output at the moment. The SPSA

TABLE 1 Algorithm parameters.

Parameters	
A	10
a	2.1127e-4
c	1e-2
α	0.602
γ	0.101
Number of iterations N	100

algorithm can calculate the optimal power share to the power grid at every sampling moment. The equation of the cost function is shown as follows.

$$y^k(\theta) = \left(\frac{q_{grid} \cdot \Delta P}{P_{grid}^{t-1}} \right)^2 \tag{18}$$

Each variable in the vector of unknown parameter θ corresponds to the distribution coefficient of the power ramp ΔP allocated to the power grid, and the hybrid storage device, as shown in the following formula.

$$\theta = [q_{grid} \quad q_{Hess}] \tag{19}$$

q_{grid} is the distribution coefficient of the grid, and q_{Hess} is the distribution coefficient of the mixed storage equipment.

Multiply the power ramp by the distribution coefficient obtained by the algorithm seeking to calculate the real-time distribution value. Then, add the power ramp allocated to the power grid with the photovoltaic power at this time to obtain the grid-connected power, as shown in the following formula.

$$P_{grid}^t = q_{grid} \times \Delta P \tag{20}$$

$$P_{Hess}^t = q_{Hess} \times \Delta P \tag{21}$$

$$P_{grid}^t = P_{grid}^t + P_{pv}^t \tag{22}$$

P_{grid}^t is the power allocated to the grid at time t , P_{Hess}^t is the power allocated to the hybrid storage device at time t , and P_{pv}^t is the power output of the photovoltaic at time t . The parameters ina_k and c_k are set according to the principle of the algorithm and the process of simulation as shown in Table 1.

TABLE 2 Power allocation strategy when $P_{HESS}(t) > 0$.

Mode	SOC of hydrogen storage			Total power of hybrid energy storage/kW			SOC of super-capacitor			AEW power	Super-capacitor power
	<0.2	[0.2,0.8]	>0.8	< P_{min}	$[P_{min},P_{max}]$	> P_{max}	<0.05	[0.05,0.95]	>0.95	/kW	/kW
1	✓			✓			✓			0	P_{HESS}
2	✓			✓				✓		P_{min}	
3			✓	✓			✓			0	P_{HESS}
4			✓	✓				✓		0	0
5	✓				✓		✓			P_{HESS}	0
6	✓				✓			✓		P_{HESS}	0
7			✓	✓			✓			0	P_{HESS}
8			✓	✓				✓		0	0
9	✓					✓	✓			P_{max}	$P_{HESS} - P_{max}$
10	✓					✓		✓		P_{max}	0
11			✓	✓			✓			0	P_{HESS}
12			✓	✓				✓		0	0

Starting from the initial value of θ , according to the principles described in Section 2.1.1, the value of distribution coefficient is obtained iteratively.

3.2.3 Application of rule control at the device level

The concentration of hydrogen in oxygen is an important indicator to measure the safety of electrolyzers in industrial production. If it is too high, it may cause explosion. For example, Fang and Liang (2019) put forward that when the rated power of electrolyzers drops to 50%, the hydrogen concentration in oxygen will drop to about 2% within 2 hours after the power drops, reaching the upper limit of safe operation of the hydrogen production system. Secondly, when the operating power is too low, the hydrogen production and power generation efficiency will be extremely low. Therefore, the power limits of hydrogen storage equipment is set within 50% to rated power. In addition, this paper constrains the SOC of the device (within 0.2–0.8 for hydrogen storage devices and 0.05–0.95 for super-capacitors), and when the SOC does not meet the constraint, the charge/discharge power is corrected to ensure that the device is within the safe operating range.

When $SOC_x(k+1) > SOC_{x,max}$, the correction formula is as follows.

$$P_x(k) = E_{x,max} \cdot \frac{SOC_x(k) - SOC_{x,max}}{\eta_x \cdot \Delta t} \quad (23)$$

x can represent hydrogen storage tank or super-capacitor. When SOC is less than the lower limit, the calculation method of the correction power is similar and will not be repeated. According to the above constraints this paper sets up

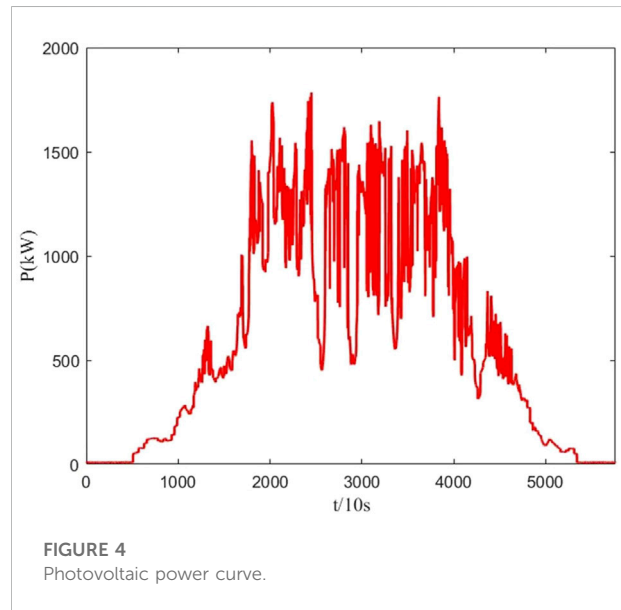
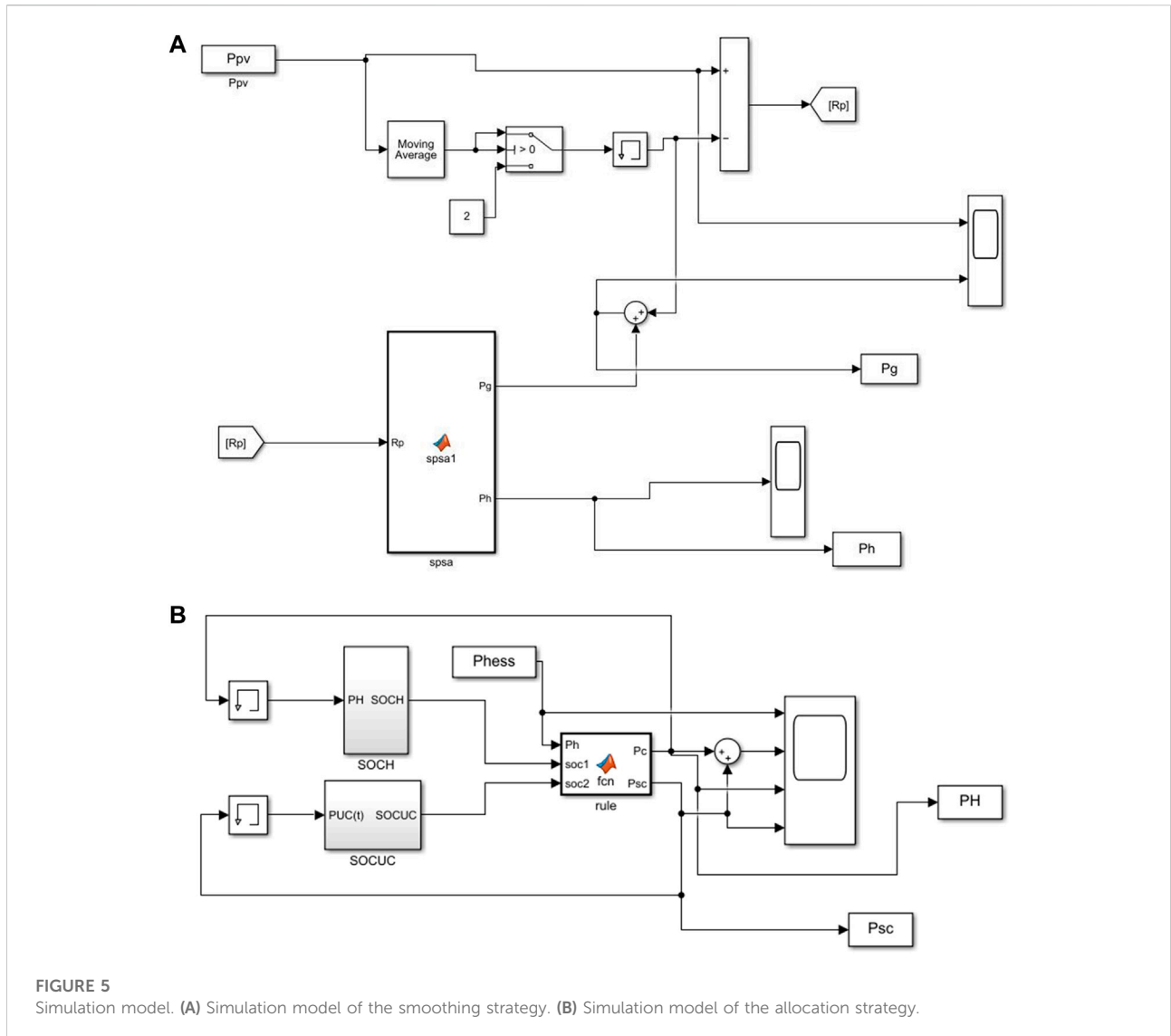


FIGURE 4 Photovoltaic power curve.

24 operation modes for the operation of hybrid energy storage system, when $P_{HESS}(t) > 0$ the allocation strategy is shown in Table 2, when $P_{HESS}(t) < 0$ the principle of allocation is the same as when $P_{HESS}(t) > 0$. Several of the typical control rules are highlighted.

Mode 1 and Mode 3: When the SOC of super-capacitor is lower than the upper limit and the total power of mixed storage is less than 200kW, the power of electrolytic cell power is set to 0 and the super-capacitor power is the total power of hybrid storage.



Mode 2: When the SOC of hydrogen storage is lower than the upper limit, the SOC of super-capacitor is higher than the upper limit and the total power of mixed storage is less than 200kW, set the power of electrolytic cell to P_{min} and the power of super-capacitor to $P_{HESS} - P_{min}$.

Mode 5 and 6: When the SOC of hydrogen storage is below the upper limit and the total power of mixed storage is between 200 and 400kW, set the power of electrolytic cell to P_{HESS} , and the power of super capacitor to 0.

Mode 9: When the SOC of hydrogen storage and super-capacitor is lower than the upper limit, and the total power of mixed storage is more than 400kw, set the power of electrolytic cell to P_{max} , and the power of super-capacitor to $P_{HESS} - P_{max}$.

Mode 10: When only the SOC of hydrogen storage is below the upper limit and the total power of mixed storage is more than

400kw, set the power of electrolytic cell to P_{max} , and the power of super-capacitor to 0.

Mode 4, 8, 12: When the SOC of both hydrogen storage and super-capacitor are over-limited, the power of both the device electrolyzer and super-capacitor is 0.

4 Example analysis

4.1 Construction of simulation model

According to the control strategy proposed in Section 2, this paper uses dataset two to build a model on MATLAB/simulink for simulation experiments. The photovoltaic power curve is shown in Figure 4. The charging and discharging efficiency of the super-capacitor is set to

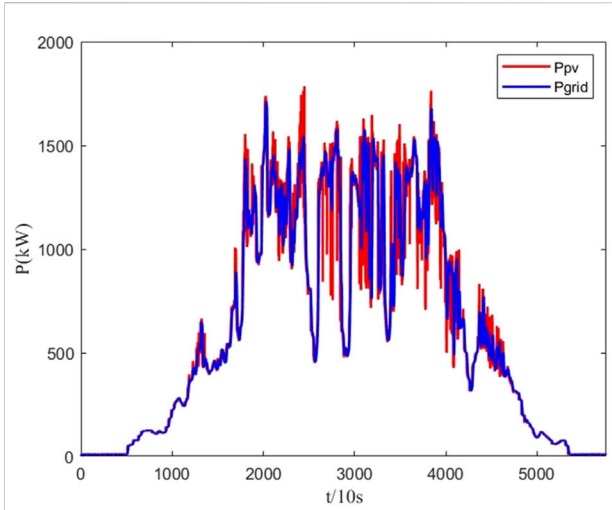


FIGURE 6
Comparison between grid-connected power calculated by SPSA and original output.

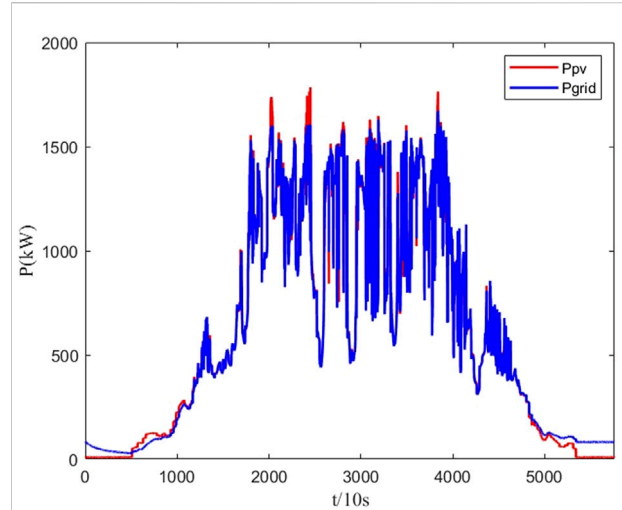


FIGURE 8
Comparison of grid-connected power calculated by RFNN and original output.

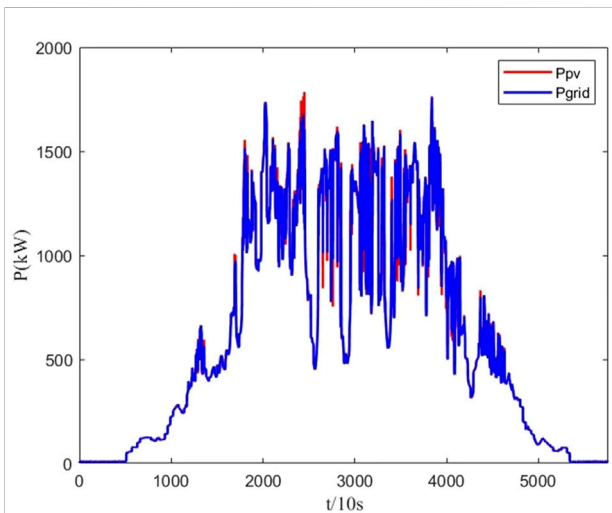


FIGURE 7
Comparison of grid-connected power calculated by low-pass filtering and original output.

95%, the charging and discharging efficiency of the electrolyzer and fuel cell is 80%, the initial SOC of the hybrid storage equipment is all 50%, and the volume of the hydrogen storage tank is 25m². In order to simplify the smoothing process, the photovoltaic output curve is first processed by the smoothing filtering method. The simulation model of the smoothing strategy is shown in Figure 5.

4.2 Analysis of smoothing results

4.2.1 Analysis of system-level smoothing fluctuation results using the simultaneous perturbation stochastic approximation algorithm

As shown in Figure 6, the simulation curve obtained by the SPSA algorithm with regular control is compared with the photovoltaic power generation. First-order low-pass filtering is an algorithm that can realize the function of hardware RC low-pass filtering by software programming, and it is widely used in practical projects. The principle is to adjust the ratio of the grid power at the previous time to the current time by adjusting the filter coefficient. RFNN is a recursive multilayer connected neural network that uses dynamic fuzzy rules to achieve fuzzy inference with online training and approximation capabilities (Teng and Lee, 2000). To verify the superiority of the algorithm, the smoothing result obtained by the algorithm, the low-pass filtering algorithm and RFNN algorithm are compared in three dimensions: the smoothness of the grid-connected power, the maximum power of the energy storage system and the maximum capacity of the hybrid energy storage system.

The stability of power network is used to measure the fluctuation range of power network. The lower the smoothness, the smaller the fluctuation of the grid power and the closer to the ideal power. The formula for calculating the smoothness is as follows.

$$D = \max \left\{ \frac{P_g(k) - P_g(k-1)}{0.1 * P_{pv \max}} \right\} \quad (24)$$

TABLE 3 Comparison of the smoothing results of the three algorithms.

Algorithm	The smoothness	The maximum power/kW	The maximum capacity ofW the hybrid energy storage system/kW.h
SPSA	0.3418	622.5968	172.4000
First-order low-pass filtering algorithm	2.9918	688.7366	49.7541
RFNN	4.2555	327.5377	103.0683

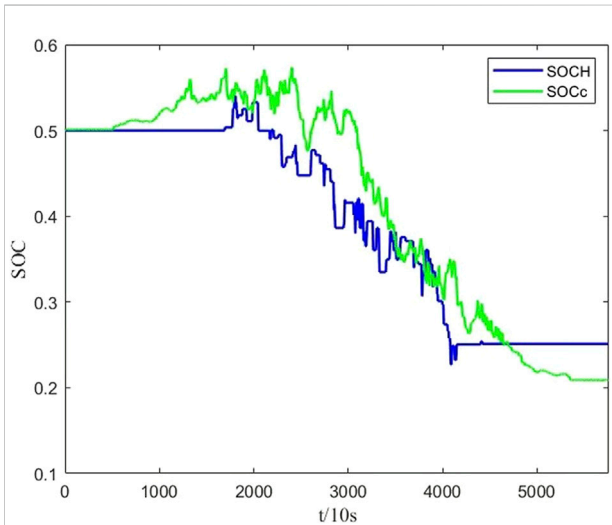


FIGURE 9 Simulation results of SOC.

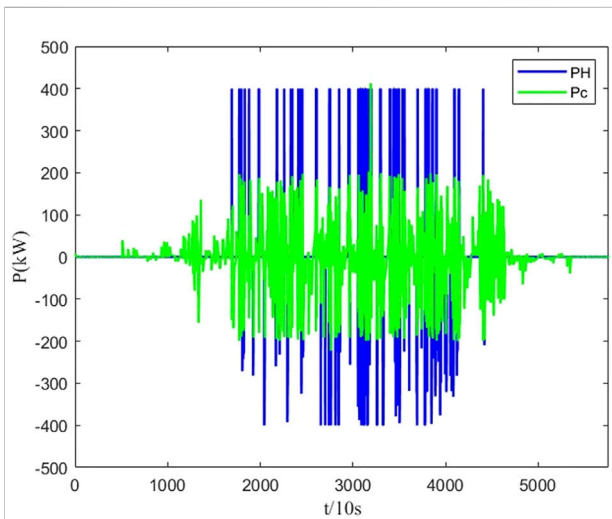


FIGURE 10 Simulation results of charge and discharge power.

where D represents the grid-connected power smoothness and $P_{pv\max}$ represents the maximum photovoltaic power.

The greater the maximum charging/discharging power of the energy storage system, the higher the investment cost. The maximum power of the energy storage system is calculated as follows.

$$P_{H\text{ESS}\max} = \max(|P_{H\text{ESS}}(k)|) \tag{25}$$

$P_{H\text{ESS}\max}$ represents the maximum power of the energy storage system.

The maximum capacity of the hybrid energy storage system is calculated as follows.

$$E_{H\text{ESS}}(k + 1) = E_{H\text{ESS}}(k) - P_{H\text{ESS}}(k)\Delta t \tag{26}$$

$$E_{H\text{ESS}\max} = \max(|E_{H\text{ESS}}|) \tag{27}$$

$E_{H\text{ESS}}(k)$ represents the total capacity of mixed storage at the k th sampling point, and, $E_{H\text{ESS}\max}(k)$ represents the maximum capacity of the hybrid energy storage device.

The results of the first-order low-pass filtering method to eliminate photovoltaic output fluctuation are shown in Figure 7, in which the filter coefficient is 0.7.

The results of smoothing photovoltaic output fluctuations using the RFNN algorithm are shown in Figure 8.

A comparison of the smoothing results of the three algorithms is shown in Table 3.

It can be seen from the table that the SPSA algorithm can greatly improve the smoothness and reduce the grid-connected power fluctuation. Compared with the first-order low-pass filtering algorithm, its maximum power fluctuation is also relatively small, but its storage capacity requirement for energy storage equipment is higher and the high energy density of hydrogen is more desirable. Second, the first-order low-pass filtering algorithm has a large time-delay characteristic because it does not predict the power at the next moment (Shi et al., 2021). Compared with the RFNN algorithm, which has at least four state parameters, its initial value setting is more complicated and easy to fall into local optimum, but the initial value setting of the SPSA algorithm is limited to the distribution coefficient, which is easy to set.

4.2.2 Analysis of device level power distribution results

Set the upper limit and the lower limit of power of electrolytic cell and fuel cell to 400 and 200 kW, respectively. The maximum pressure of the hydrogen storage tank is 10 kPa and the maximum capacity of the super-capacitor is 166 kWh. The SOC simulation results of two kinds of energy storage devices are shown in Figure 8. SOC_H is the SOC of hydrogen storage, and SOC_C is the SOC of super capacitor. From the figure, it can be seen that the SOC of super-capacitor and hydrogen storage are complementary in some time periods. The simulation results of charging and discharging power are as shown in Figure 9.

It can be seen that the rule control can keep the charging and discharging power of the hydrogen storage device within the range of rated power and safe operation as much as possible, and because the rule is fixed, the hydrogen storage device can avoid frequent start and stop and rapid high-frequency fluctuations mainly caused by super capacitor.

5 Conclusion

- 1) The SPSA algorithm with real-time control is used to smooth the fluctuation of photovoltaic power output. Compared with the first-order low-pass filtering algorithm and RFNN algorithm, SPSA algorithm has more remarkable ability to smooth photovoltaic power, and has greater robustness.
- 2) The power of hybrid energy storage is distributed by the method of rule control, so that the fuel cell and electrolytic cell can work between the rated power and the minimum working power as much as possible, and the SOC of the hybrid energy storage equipment is taken into account at the same time, so that the energy storage equipment can work in a safe range.
- 3) The model is built and simulated using simulation software, which verifies the effectiveness of the proposed strategy and has some practical significance.

References

- Akbari, H., Browne, M. C., Ortega, A., Huang, M. J., Hewitt, N. J., Norton, B., et al. (2019). Efficient energy storage technologies for photovoltaic systems. *Sol. Energy* 192, 144–168. doi:10.1016/j.solener.2018.03.052
- Barelli, L., Ciupageanu, D.-A., Ottaviano, A., Pelosi, D., and Lazaroiu, G. (2020). Stochastic power management strategy for hybrid energy storage systems to enhance large scale wind energy integration. *J. Energy Storage* 31, 101650. doi:10.1016/j.est.2020.101650
- Bharti, N., Kumar, S., and Chawla, P. (2022). *Sizing and optimization of hybrid energy storage system with renewable energy generation plant*. Singapore: Springer Nature Singapore.
- Castillo, A. G., and Dennice, F. (2014). Grid-scale energy storage applications in renewable energy integration: A survey. *Energy Convers. Manag.* 84, 885–894. doi:10.1016/j.enconman.2014.07.063
- Fang, R., and Liang, Y. (2019). Control strategy of electrolyzer in a wind-hydrogen system considering the constraints of switching times. *Int. J. Hydrog. Energy* 44 (46), 25104–25111. doi:10.1016/j.ijhydene.2019.03.033
- Li, C. Z. a. X. (2021). “A novel real-time energy management strategy for grid-friendly microgrid: Harnessing internal fluctuation internally,” in *2020 52nd north American power symposium (NAPS) tempe*, 1–6.
- Li, P., Duan, Q., Li, Z., Zhu, C., and Zhang, X. (2020). A Lyapunov optimization-based energy management strategy for energy hub with energy router. *IEEE Trans. Smart Grid* 11, 4860–4870. doi:10.1109/tsg.2020.2968747
- Mokkadem, A., and Pelletier, M. (2007). A companion for the Kiefer–Wolfowitz–Blum stochastic approximation algorithm. *Ann. Statist.* 35 (4), 1749–1772. doi:10.1214/009053606000001451
- Neely, M. J., Saber Tehrani, A., and Dimakis, A. G. (2010). “Tehrani, Arash Saber; Dimakis, Alexandros GEfficient algorithms for renewable energy allocation to delay tolerant consumers,” in *2010 first IEEE international conference on Smart grid communications* (Los Angeles, CA, United: University of Southern California), 549–554. doi:10.1109/SMARTGRID.2010.5621993
- Nigam, A., and Sharma, K. K. (2021). “Modeling Approach for different solar PV system: A review,” *Advances in systems, control and automations*. Editors

Data availability statement

The raw data supporting the conclusions of this article will be made available by the authors, without undue reservation.

Author contributions

All authors listed have made a substantial, direct, and intellectual contribution to the work and approved it for publication.

Funding

The work is supported by the central government guides local special funds for science and technology development under ZYYD2022B11.

Conflict of interest

The authors declare that the research was conducted in the absence of any commercial or financial relationships that could be construed as a potential conflict of interest.

Publisher's note

All claims expressed in this article are solely those of the authors and do not necessarily represent those of their affiliated organizations, or those of the publisher, the editors and the reviewers. Any product that may be evaluated in this article, or claim that may be made by its manufacturer, is not guaranteed or endorsed by the publisher.

- A. K. Bhoi, P. K. Mallick, V. E. Balas, and B. S. P. Mishra (Singapore: Springer), Vol. 435. doi:10.1007/978-981-15-8685-9_70
- Puranen, P. K., Antti, K., and Ahola, J. (2021). Technical feasibility evaluation of a solar PV based off-grid domestic energy system with battery and hydrogen energy storage in northern climates. *Sol. Energy* 213, 246–259. doi:10.1016/j.solener.2020.10.089
- Shaner, M. R., Davis, S. J., Lewis, N. S., and Caldeira, K. (2018). Geophysical constraints on the reliability of solar and wind power in the United States. *Energy Environ. Sci.* 11, 914–925. doi:10.1039/C7EE03029K
- Shi, X., Zhao, Y., Zhang, H., Wang, X., and Zhou, B. (2021). Control method of wind power fluctuation smoothing for battery energy storage system based on quasi-zero phase filter. *Automation Electr. Power Syst.* 45 (4), 45–53.
- Spall, J. C. (1997). A one-measurement form of simultaneous perturbation stochastic approximation. *Automatica* 33 (1), 109–112. doi:10.1016/S0005-1098(96)00149-5
- Tabar, V. S., Saeid, G., and Tohidi, S. (2019). Energy management in hybrid microgrid with considering multiple power market and real time demand response. *Energy* 174, 10–23. doi:10.1016/j.energy.2019.01.136
- Teng, C.-C., and Lee, C.-H. (2000). Identification and control of dynamic systems using recurrent fuzzy neural networks. *IEEE Trans. Fuzzy Syst.* 8, 349–366. doi:10.1109/91.868943
- Wang, M., Xiaobin, D., and Zhai, Y. (2021). Optimal configuration of the integrated charging station for PV and hydrogen storage. *Energies* 14 (21), 7087. doi:10.3390/en14217087
- Wang, S., and Lin, H. (2019). Control strategy of hybrid energy storage to stabilize wind power fluctuation based on variable coefficient exponential smoothing method. *Acta Energ. Sol. Sin.* 40 (11), 3204–3212. doi:10.1016/j.rser.2017.05.283
- Wu, Y., Chrenko, D., and Miraoui, A. (2018). “A real time energy management for EV charging station integrated with local generations and energy storage system,” in *2018 IEEE transportation electrification conference and expo (ITEC)*, 1–6.
- Yin, S., Li, J., Li, Z., and Fan, S. (2021). Energy pricing and sharing strategy based on hybrid stochastic robust game approach for a virtual energy station with energy cells. *IEEE Trans. Sustain. Energy* 12, 772–784. doi:10.1109/tste.2020.3019494
- Zhang, L., Hu, X. S., Wang, Z. P., Sun, F. C., and Dorrell, D. G. (2018). A review of super-capacitor modeling, estimation, and applications: A control/management perspective. *Renew. Sustain. Energy Rev.* 81, 1868–1878. doi:10.1016/j.rser.2017.05.283

Nomenclature

Variables

P Power

N Flow rate

U Voltage

E Capacity

F Faraday constant

η Efficiency

D Grid-connected power smoothness

q Weighting of power ramp allocation

θ The distribution factor of the power ramp ΔP

Subscripts

pv Photovoltaic

grid Grid-connected

HES Hybrid energy storage system

c Super-capacitor

H Hydrogen storage system

C Charge

D Discharge

AEW Alkaline electrolyzed water

FC Fuel cell

Abbreviations

RFNN recursive fuzzy neural network

SPSA simultaneous perturbation stochastic approximation

SOC State of charge